Parasitic Effects of Grounding Paths on Common-Mode EMI Filter's Performance in Power Electronics Systems

Shuo Wang, *Senior Member, IEEE*, Yoann Yorrick Maillet, Fei Wang, *Fellow, IEEE*, Rixin Lai, *Member, IEEE*, Fang Luo, *Student Member, IEEE*, and Dushan Boroyevich, *Fellow, IEEE*

***Abstract*—High-frequency common-mode (CM) electromagnetic-interference (EMI) noise is difficult to suppress in electronics systems. EMI filters are used to suppress CM noise, but their performance is greatly affected by the parasitic effects of the grounding paths. In this paper, the parasitic effects of the grounding paths on an EMI filter's performance are investigated in a motor-drive system. The effects of the mutual inductance between two grounding paths are explored. Guidelines for the grounding of CM EMI filters are derived. Simulations and experiments are finally carried out to verify the theoretical analysis.**

***Index Terms*—Electromagnetic-interference (EMI) filter, grounding, inductive coupling, motor drive, mutual inductance, parasitic.**

I. Introduction

ELECTROMAGNETIC emission can be generated from switch-mode power conversion systems. Electromagnetic emission is conventionally categorized as either differential-mode (DM) or common-mode (CM) noise. DM noise is the noise current flowing within the power delivery paths, while CM noise is the noise current flowing between the ground and the power circuits. DM and CM emissions are usually called electromagnetic-interference (EMI) noise. EMI filters are widely used in power electronics systems to suppress electromagnetic emission. A typical EMI filter composed of DM and CM filters is shown in Fig. 1. The DM capacitors (C_1, C_2, and C_3) and CM capacitors (C_{CM1} and C_{CM2}) have low impedance. They are in the noise' shunt paths so they can bypass the EMI noise. The DM inductors (L_{DM1} and L_{DM2}) and CM inductors (L_{CM1} and L_{CM2}) have high impedance and are in the noise's series paths so they can block the EMI noise. The DM inductance can be the leakage of the CM inductor, but when the leakage is not enough, two separate DM inductors, represented by the L_{DM1} shown in Fig. 1, are usually needed. Two identical inductors on the left stage are not coupled; therefore, CM inductance L_{CM2} is half of the inductance of a single inductor, and DM inductance L_{DM2} is twice that of the inductance of a single inductor. These two filter stages can target the entire interested frequency range or one stage can be used for low frequencies and the other for high frequencies. In the filter discussed in this paper, the first (right) stage targets the low-frequency noise attenuation, and the second (left) stage targets the high-frequency (HF) noise reduction.

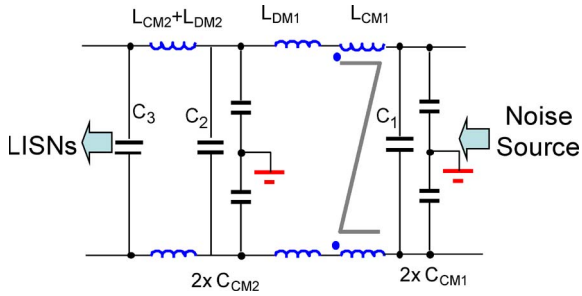

Fig. 1. Conventional EMI filter used in power electronics systems.

An application of EMI filters in a motor-drive system is shown in Fig. 2. In the system in Fig. 2, CM noise current is generated by the switching of the power switches and the parasitic capacitance between the ground and the motor-drive system. The CM parasitic capacitance includes the parasitic capacitance C_G in the motor, the parasitic capacitance C_{SHIELD} (not shown in the figure) between the inner conductors and the shield of the cable, and the parasitic capacitance $6 \times C_{CH}$ between the switches and the heat sink. The heat sink and the chassis of the motor drive are directly grounded and set on the ground plane. The frame of the motor is grounded via the shield of the cable and the chassis of the motor drive. The CM noise current from the motor and the cable is I_{CM1}, and the CM current from the heat sink is I_{CM2}. I_{CM3} and I_{CM4} are the CM currents bypassed by the $2 \times C_{CM1}$ and $2 \times C_{CM2}$ in the EMI filter. Two line impedance stabilization networks (LISNs) are used on the dc input side for EMI measurement. The conventional design procedure for the CM EMI filter does

Manuscript received May 12, 2009; revised August 14, 2009 and October 7, 2009; accepted November 8, 2009. Date of publication December 4, 2009; date of current version August 11, 2010. This work was supported by the SAFRAN Group.

S. Wang is with Department of Electrical and Computer Engineering, The University of Texas at San Antonio, San Antonio, TX 78249-1644 USA (e-mail: shuowang@ieee.org).

Y. Y. Maillet is with Converteam, Inc., Pittsburgh, PA 15238 USA (e-mail: yoayo@vt.edu).

F. Wang is with The University of Tennessee, Knoxville, TN 37996 USA, and also with Oak Ridge National Laboratory, Oak Ridge, TN 37830-8050 USA (e-mail: fred.wang@utk.edu).

R. Lai is with the GE Global Research Center, General Electric Company, Niskayuna, NY 12309 USA (e-mail: lairixin@vt.edu).

F. Luo is with Huazhong University of Science and Technology, Wuhan 430074, China (e-mail: kkhust@gmail.com).

D. Boroyevich is with the Center for Power Electronics Systems and the Department of Electrical and Computer Engineering, Virginia Polytechnic Institute and State University, Blacksburg, VA 24061-0179 USA (e-mail: dushan@vt.edu).

Color versions of one or more of the figures in this paper are available online at http://ieeexplore.ieee.org.

Digital Object Identifier 10.1109/TIE.2009.2037643

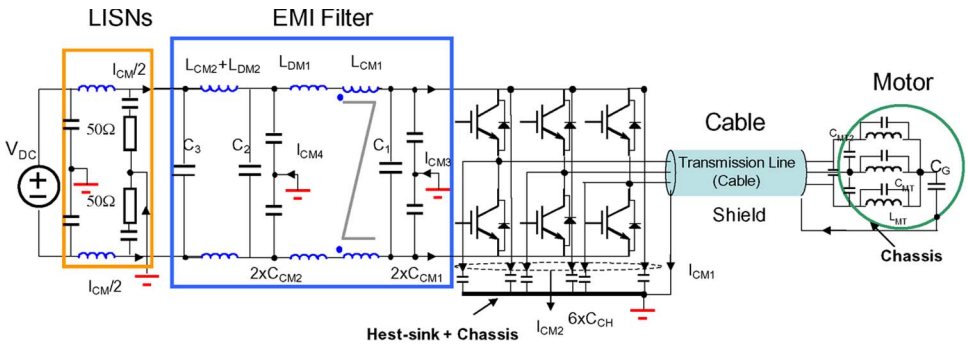

Fig. 2. EMI filter in a motor-drive system.

not consider the effects of the parasitics in the filter's grounding paths. However, in practical cases, the self- and mutual parasitics and grounding patterns have a big impact on a CM EMI filter's performance. Existing literature, such as [3]–[5] and [8]–[10], discuss grounding in general without addressing and analyzing specific applications, such as EMI filters. Reference [17] presents some important experimental analysis of the effects of the grounding loops. Reference [7] discusses EMI filters but never theoretically analyzes and quantifies the parasitic effects of grounding paths on CM noise suppression. Furthermore, a very important issue, the mutual inductance between two grounding paths, has not been addressed in the existing literature.

This paper will discuss the parasitic effects of grounding paths on a CM EMI filter's performance. The effects of self- and mutual parasitics on a CM filter's performance will be discussed with different grounding patterns. The parasitic effects will be theoretically analyzed and verified in experiments. Some guidelines for efficient grounding are derived.

II. Analysis of Parasitic Effects of Grounding Paths

Reference [9] gives some general guidelines on single- and multipoint grounding for an electronic system. This chapter will focus on the theoretical analysis of the effects of parasitics in grounding paths. The effects of the mutual inductance between different grounding paths, which is not investigated in the past literature, will be investigated. Some guidelines on the design of CM filters will be derived based on the analysis.

A. Effects of Self-Parasitics of Grounding Paths on CM Filter's Performance

For the system in Fig. 2, the CM noise model including only the self-parasitics of filter components can be shown in Fig. 3. In Fig. 3, the impedance of the ground plane is ignored, and the CM noise source can be simply modeled using Thevenin's theorem. V_{CM} represents the equivalent CM noise voltage source, while C_S and Z_S represent the equivalent series impedances. C_S models the effects of CM parasitic capacitance, and Z_S represents the other effects of parasitics in a CM noise source. $ESL_{CM1}/2$ and $ESL_{CM2}/2$ are the equivalent series inductances of capacitors $2 \times C_{CM1}$ and $2 \times C_{CM2}$, and EPC_1 and EPC_2 are the equivalent parallel capacitances of

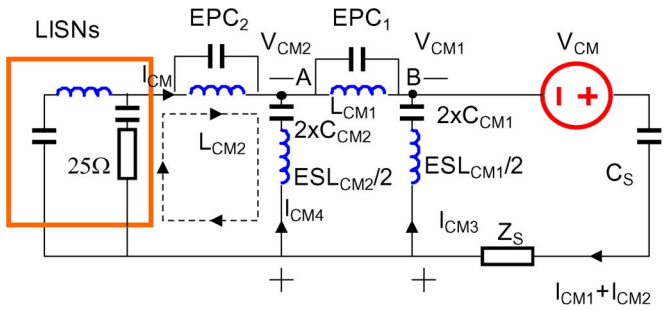

Fig. 3. CM noise model including only the self-parasitics of filter components.

CM inductors L_{CM1} and L_{CM2}. In Fig. 3, the left side is the model of the LISNs. The CM noise flowing through LISNs is defined as

$$I_{CM} = (I_{CM1} + I_{CM2}) - (I_{CM3} + I_{CM4}). \tag{1}$$

It should be noted that, based on the ideal LC filter's characteristics, the noise voltage V_{CM1} between the ground and point B in Fig. 3 is much larger than the noise voltage V_{CM2} between the ground and point A. These voltages differ by 40 dB/dec. The difference of the currents I_{CM3} and I_{CM4} in the two CM capacitor branches is similar. V_{CM2} is added to the filter's output loop. A higher V_{CM2} leads to a higher CM noise measured on the LISNs. V_{CM2} is defined in

$$V_{CM2} = \frac{I_{CM4}}{2}\left[j\omega ESL_{CM2} + \frac{1}{j\omega C_{CM2}}\right]. \tag{2}$$

For a practical printed circuit board (PCB) layout for EMI filters, there is a large piece of copper plane on the PCB to which all the CM capacitors are soldered. The copper plane is grounded to the ground plane via the chassis of the system or a separate grounding path. The noise model can be shown in Fig. 4. In Fig. 4, L_P is the parasitic inductance of the grounding path from the copper plane to the ground plane. Z_{GP} is the impedance of the ground plane between the LISNs and the grounding point. Since Z_{GP} is in the CM noise' series paths, its impedance does not make the CM noise worse. For source impedances C_S and Z_S, the situation is a little bit different, because there may be a series resonance in the input loop. If this resonance is within the frequency range of interest, there will be a noise peak observed.

The effects of the self-parasitics in the grounding paths on the filter's performance can be analyzed by examining Fig. 4.

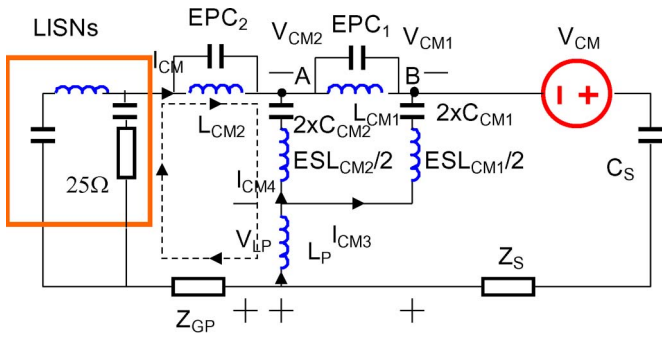

Fig. 4. CM noise model with the parasitic inductance L_P on the grounding path.

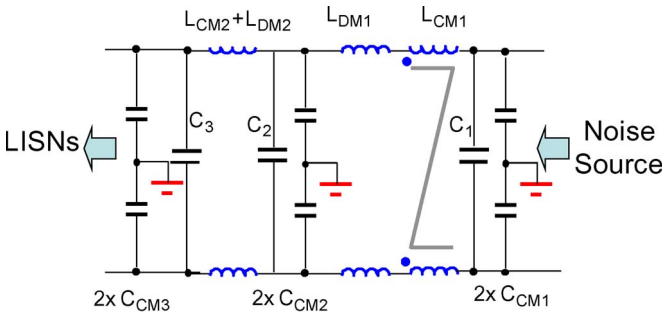

Fig. 5. EMI filter with a π-type CM filter on the second stage.

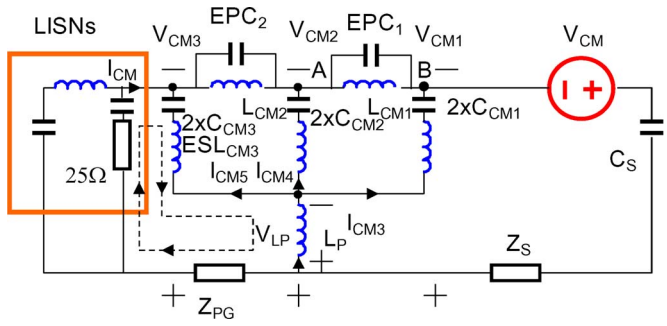

Fig. 6. CM equivalent circuit for the filter with CM capacitors on the output loop.

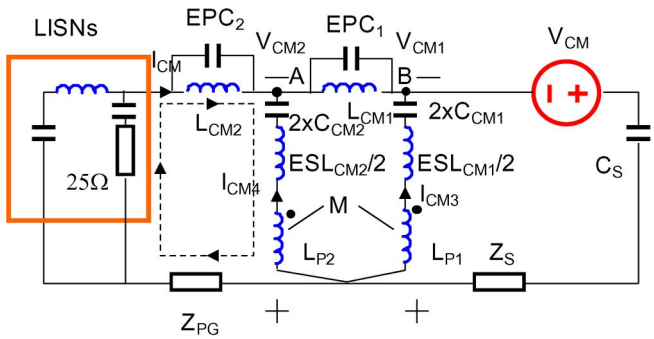

Fig. 7. CM capacitors on each stage are grounded separately.

In Fig. 4, both CM currents in I_{CM3} and I_{CM4} flow through L_P. They have a voltage drop V_{LP} on L_P. V_{LP} and V_{CM2} are given by (3) and (4), respectively,

$$V_{\rm LP} = j\omega L_P(I_{\rm CM4} + I_{\rm CM3}) \tag{3}$$

$$V_{\rm CM2} = \frac{I_{\rm CM4}}{2}\left(j\omega ESL_{\rm CM2} + \frac{1}{j\omega C_{\rm CM2}}\right) + V_{\rm LP}. \tag{4}$$

As stated before, I_{CM3} is much larger than I_{CM4}. L_P could be much larger than $ESL_{CM2}/2$ of the CM capacitors. The V_{CM2} in (4) is thus much larger than the V_{CM2} in (2) at high frequencies. At high frequencies, at which the impedance of $2 \times C_{CM2}$ can be ignored, the ratio n of the second term to the first term in (4) is given by

$$n \approx \frac{2I_{\rm CM3}L_P}{I_{\rm CM4}ESL_{\rm CM2}}. \tag{5}$$

From (5), it can be seen that, if I_{CM3} were 100 times I_{CM4} and L_P were five times ESL_{CM2}, there would be a 60-dB degradation on the CM filter's performance. Reducing L_P (for example, by using a copper strip) would be helpful for reducing n, but its improvement strongly depends on the difference of I_{CM3} and I_{CM4}. It can be derived that using more CM capacitors at the output of the CM filter may increase CM noise instead of reducing it. As an example, if there are two more CM capacitors $2 \times C_{CM3}$ on the output of the filter, as shown in Fig. 5, the CM noise model can be shown in Fig. 6.

In Fig. 6, after adding two CM capacitors (noted as $2 \times C_{CM3}$) to the output of the filter, the noise V_{LP} is directly added to the LISNs via these two CM capacitors. Since the impedance of $2 \times C_{CM3}$ is much smaller than the impedance of the CM inductor L_{CM2} at high frequencies, by adding $2 \times C_{CM3}$, the output loop impedance is smaller than that without $2 \times C_{CM3}$, which means that the measured CM noise on the LISNs is higher than it would be without $2 \times C_{CM3}$.

In order to avoid the issues discussed previously in multistage EMI filters, CM capacitors on each stage should be grounded separately. Soldering all CM capacitors to the same copper plane on the PCB is not a good idea. If the CM capacitors have to share the same grounding path, the output loop should not have CM capacitors.

B. *Effects of Mutual Inductance Between Grounding Paths on CM Filter's Performance*

As analyzed in the previous section, if the CM capacitors on each stage are grounded separately, the issue caused by the self-parasitics described previously is eliminated. However, experiments show that the improvement of the CM filter's performance is still limited. Further investigation disclosed that the mutual inductance between different grounding paths plays a very important role. Fig. 7 shows a CM noise model including a filter with mutual inductance M between two grounding paths.

In Fig. 7, the two grounding paths have the parasitic inductances L_{P1} and L_{P2}, respectively. The I_{CM3} in L_{P1} would not flow through L_{P2}; thus, the issue discussed previously in the case of the shared grounding path no longer exists. However, as analyzed in Section II-A, at high frequencies, the CM noise current I_{CM4} is much smaller than I_{CM3}, and the voltage V_{CM2} is much smaller than V_{CM1}; hence, a very small mutual inductance between L_{P1} and L_{P2} will induce a significant voltage on L_{P2}. The equivalent circuit used for analysis after two grounding paths are decoupled is shown in Fig. 8.

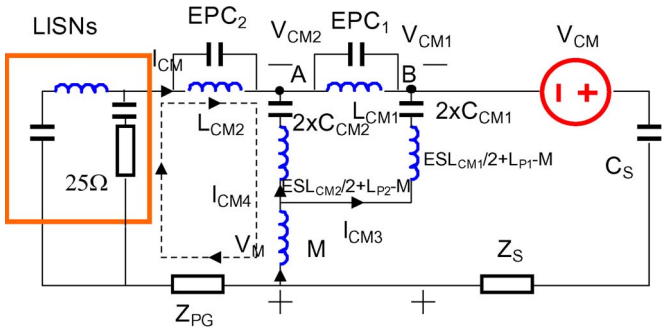

Fig. 8. CM equivalent circuit for the filter with separate grounding paths.

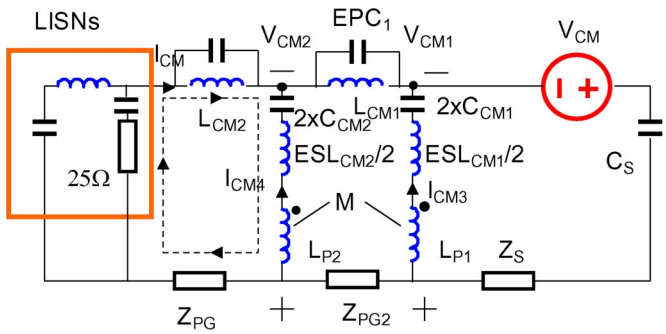

Fig. 9. CM capacitors of each stage are grounded separately at two points on the ground plane.

In Fig. 8, the effects of the mutual inductance between the two grounding paths are represented by a shared grounding path with an inductance of M. $\mathrm{V_{CM2}}$ with the effects of M can be given by (6) and (7)

$$V_M = j\omega M(I_{\mathrm{CM4}} + I_{\mathrm{CM3}}) \tag{6}$$

$$V_{\mathrm{CM2}} = \frac{I_{\mathrm{CM4}}}{2}\left[j\omega\left[ESL_{\mathrm{CM2}} + 2(L_{P2} - M)\right] + \frac{1}{j\omega C_{\mathrm{CM2}}}\right] + V_M \tag{7}$$

$$n \approx \frac{M}{ESL_{\mathrm{CM2}}/2 + (L_{P2} - M)}\left(\frac{I_{\mathrm{CM3}}}{I_{\mathrm{CM4}}}\right) \tag{8}$$

$$\left|\frac{I_{\mathrm{CM3}}}{I_{\mathrm{CM4}}}\right| > \frac{1}{M}(ESL_{\mathrm{CM2}}/2 + L_{P2} - M). \tag{9}$$

Following a similar analysis to the case in Section II-A, at high frequencies, at which the impedance of $2 \times \mathrm{C_{CM2}}$ can be ignored and $\mathrm{I_{CM3}}$ is much larger than $\mathrm{I_{CM4}}$, the ratio n of the second term to the first term in (7) is given by (8). In (8), the effect of M is equivalently amplified by $\mathrm{I_{CM3}}/\mathrm{I_{CM4}}$ times. As an example, if M is only 1% of the equivalent inductance of the grounding path represented in the denominator, a difference of more than 40 dB between $\mathrm{I_{CM3}}$ and $\mathrm{I_{CM4}}$ would make the effects of mutual inductance dominant. Equation (9) describes the condition that the current ratio between $\mathrm{I_{CM3}}$ and $\mathrm{I_{CM4}}$ is larger than the inductance ratio in (8). Before mutual inductance M plays a major role in the CM filter's performance, $\mathrm{I_{CM3}}$ is much larger than $\mathrm{I_{CM4}}$, and their difference increases when frequency increases. At a certain frequency f_1 determined by the inductance ratio in (9), the condition is met, and M begins to play a major role above this frequency. Based on (9), the higher M is, the lower the frequency f_1 is and, therefore, the worser the filter's performance is at high frequencies. On the contrary, the smaller M is, the higher f_1 is and, hence, the better the filter's performance is at high frequencies. If the inductance of the grounding path is minimized so that $\mathrm{L_{P2}}$ and M are much smaller than $\mathrm{ESL_{CM2}}/2$, the filter's performance would be good at a very wide frequency range since f_1 is very high. M and $\mathrm{L_{P2}}$ should therefore be as small as possible to reduce the $\mathrm{V_{CM2}}$ and improve the filter's HF performance.

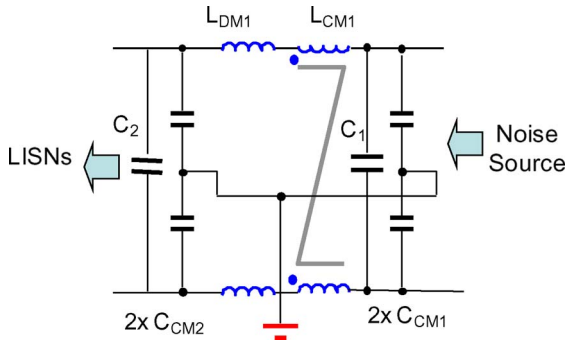

Fig. 10. One-stage π-type EMI filters.

It should be noted that the effects of the mutual capacitance between the two grounding paths is not as significant as the mutual inductance since the grounding paths have much lower impedances than that of the mutual capacitance (for example, 100 nH versus 10 pF) within the conducted EMI frequency range.

There are several ways to reduce M. For example, the two grounding paths should be as far apart as possible. CM capacitors can be separately grounded to the closest points on the ground plane with short grounding wires. The mutual inductance can be reduced by these two ways since the mutual inductance is proportional to the length of grounding wire and inversely proportional to the distance of the two grounding paths. Fig. 9 shows the CM noise model for the case of separate grounding.

In Fig. 9, $\mathrm{Z_{PG2}}$ is the impedance of the ground plane between the two grounding points. The effects of this impedance can be ignored since it is in series with CM inductor $\mathrm{L_{CM1}}$ and is very small. Since $\mathrm{Z_{PG2}}$ can be ignored, the two grounding paths are connected together via the ground plane. Because of this, it can be analyzed using the same equivalent circuit shown in Fig. 8. Since M is much smaller than that in the previous case, the CM filter's performance is greatly improved at high frequencies.

The aforementioned analysis can be applied to any filter structures, such as the one-stage EMI filter in Fig. 10. In Fig. 10, if two sets of CM capacitors share the same grounding path, removing $2 \times \mathrm{C_{CM2}}$ may yield lower CM noise. If $2 \times \mathrm{C_{CM2}}$ must be used, they should be grounded far away from $2 \times \mathrm{C_{CM1}}$.

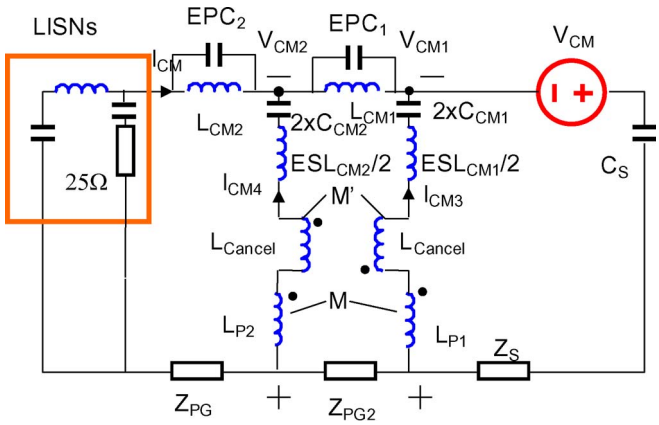

Fig. 11. Cancellation of mutual inductance between two grounding paths.

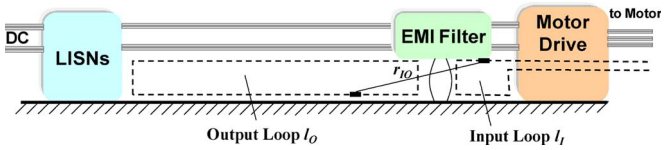

Fig. 12. Input and output CM noise loops.

The inductive mutual coupling between two grounding paths can also be reduced using other methods, for example, using two coupled inductors L_{Cancel} shown in Fig. 11 on two grounding paths to cancel the mutual inductance M between two grounding paths. The mutual inductance M' of the coupled inductors have the same value as the M between two grounding paths but with different coupling polarities. The total effects would be the cancellation. The best scenario would be when the inductance of two coupled inductors is equal to M and their coupling coefficient is equal to 1. The cancellation inductor, would not increase the inductance of the grounding path much.

C. Physical Meaning of Self- and Mutual Inductance of Grounding Paths

The mutual inductance M and self-inductances L_{P1} and L_{P2} are lumped parameters for the convenience of analysis. It is necessary to understand what they represent. In practical cases, the inductive couplings exist between the input and output CM noise loops. Fig. 12 shows the input loop l_I and output loop l_O. r_{IO} is the distance between any two current segments on two loops. The mutual inductance M between these two loops can be found via the Neumann theory in

$$M = \frac{\mu_0}{4\pi} \oint_{l_O} \oint_{l_I} \frac{dl_I \bullet dl_O}{r_{IO}}. \tag{10}$$

To further analyze the inductive couplings between the input and output CM noise loops, self partial inductance and mutual partial inductance [18] are introduced to the CM noise equivalent circuit in Fig. 13. Because only the inductive couplings between two CM noise loops are to be analyzed, other components including impedances and noise voltage source are not shown and analyzed here. In Fig. 13, each side of the input and output loops is represented with a decoupled inductance. This

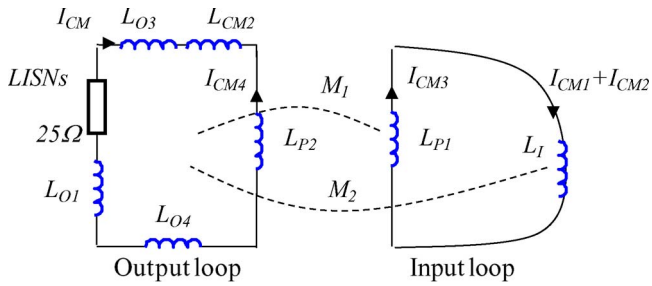

Fig. 13. Mutual partial inductance between CM noise input and output loops.

decoupled inductance includes the effects of both the self partial inductance of that side and the mutual partial inductances within that loop. L_{P1} and L_{P2} represent the decoupled inductance of two grounding paths in the input and output loops, respectively. L_I includes the decoupled inductance between the grounding point of the EMI filter and the grounding point of the motor-drive system, the inductance between the EMI filter and the insulated-gate bipolar transistors (IGBTs) in the motor drive, and the inductance of the cable and the motor. L_I's value depends on the dimensions and structures of the motor drive, cable, and motor. L_{O4} represents the decoupled inductance of the ground plane between the grounding point of the EMI filter and the grounding point of LISNs. For an ideal ground, it should be zero. L_{O1} represents the decoupled inductance of LISNs. L_{O3} represents the decoupled inductance of the dc bus between the EMI filter and the LISNs. L_{O3} is strongly related to measurement setups. There is a mutual partial inductance M_1 between L_{P1} and the output loop and a mutual partial inductance M_2 between L_I and the output loop. The mutual inductance M between two loops in the previous analysis is the sum of M_1 and M_2. The possible couplings related to filter components will be discussed later in Section III.

In Fig. 13, since most of the CM noise current from the CM noise source is bypassed by CM capacitors $2 \times C_{CM1}$, I_{CM3} is very close to the CM noise $I_{CM1} + I_{CM2}$. The induced voltages in the output loop are in series; therefore, they add together. The total induced voltage V_M is given by (11), and it increases the measured CM noise on LISNs

$$V_M \approx j\omega I_{CM3}(M_1 + M_2) = j\omega I_{CM3} M. \tag{11}$$

Physically, L_{P1} is closer to the output loop than L_I. Based on Neumann theory in (10), the mutual partial inductance is inversely proportional to the distance between two current segments, so M_1 could contribute to most of M depending on the distance between two grounding paths, the system structure, and the measurement setup. If two pairs of CM capacitors in Fig. 1 share one grounding path, M_1 reaches its maximum because most of the magnetic flux generated by I_{CM3} links the output loop. In that case, M_1 is close to L_{P1} and L_{P2}. Changing the length and the distance of two grounding wires will directly change M_1. The diameter of the grounding wires will play an important role on M_1 only when the distance is small or a shared grounding path is used. On the other hand, changing the length and the distance of two grounding wires may not change M_2 as significantly as M_1, since the other parts of the system are kept intact.

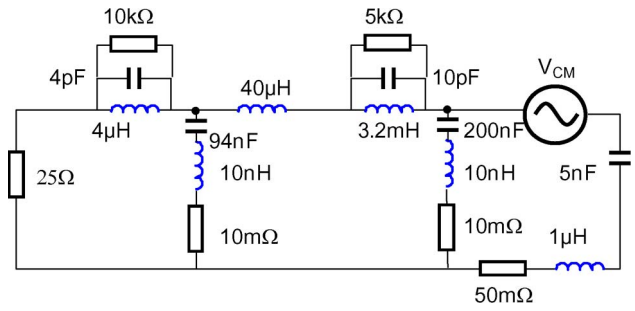

Fig. 14. CM filter model used in simulation.

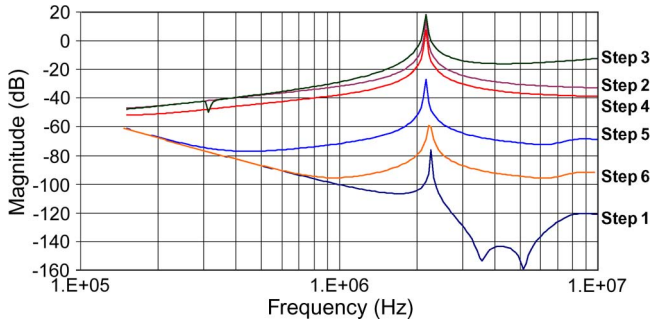

Fig. 15. Simulated insertion gains.

Based on the aforementioned analysis, L_{P1} and L_{P2} represent the decoupled inductances of two grounding paths, including the effects of mutual partial inductance within the input and output loops. M represents the mutual inductance between input and output loops. M is lumped as the mutual inductance between L_{P1} and L_{P2} because it has the same parasitic effects on the output loops as the original. The aforementioned analysis also indicates that, if the distance between two grounding paths is small, the mutual inductance between two loops with separated grounding paths would be close to that with a shared grounding path. As a result, the improvement of separating grounding paths is small.

III. Simulations and Experimental Results

The analysis in Section II is first verified by simulations. The circuits in Figs. 3, 4, 6, 7, and 9 are simulated in Pspice. Fig. 3 is redrawn in Fig. 14. All component values used in simulations are shown in Fig. 14. In Fig. 14, the 40-μH inductance represents the effects of the leakage inductance of the two CM inductor windings and the two DM inductors L_{DM1} on CM noise in Fig. 1. In the first step, there are no parasitics in the grounding path. The insertion gain is simulated and shown in Fig. 15. In the second step, the insertion gain is simulated for the circuit in Fig. 4, where L_P, the parasitic inductance of the grounding path, is 100 nH. The insertion gain is much worse, particularly at high frequencies, than the insertion gain of the filter without any parasitics in the grounding path. The peak between 2 and 3 MHz is caused by the series resonance in the input loop, as analyzed in Section II. In the third step, the insertion gain for the circuit in Fig. 6 is simulated, where C_{CM3} is 100 nF and ESL_{CM3} is 10 nH. As expected, the insertion gain is worse than that in Step 2 since the two CM capacitors provide a shortcut for the CM noise on the grounding path. In the fourth step, the insertion gain for the circuit in Fig. 7 is simulated, where L_{P1} is 100 nH, L_{P2} is 100 nH, and the coupling coefficient is 0.5 (M is 50 nH). Although the two CM capacitor branches are grounded separately, the filter has only a few decibels of improvement due to the inductive couplings between two paths. In the fifth step, the insertion gain for the circuit in Fig. 7 is simulated again but with a much smaller coupling coefficient of 0.01 (mutual inductance M is 1 nH). The filter has an improvement of more than 30 dB since the mutual inductance is much smaller than that in Step 4. In the last step, the insertion gain for the circuit in Fig. 9 is simulated, where L_{P1} is 20 nH, L_{P2} is 20 nH, and the coupling coefficient is only 0.003 (M is 0.06 nH). The mutual inductance is smaller than that in Step 5. The filter has another 24-dB improvement. These simulation results verify the analysis in Section II. It should be pointed out that the purpose of simulation is just to verify the theoretical analysis. Therefore, not every parasitic parameter used in the simulation is the same as the actual in-circuit values.

Experiments are finally carried out in a motor-drive system to verify the analysis in Section II. A two-stage EMI filter is built with a similar structure to that shown in Fig. 1 except that the inductors in the second stage are two separate inductors instead of a coupled inductor. The separate inductors have impedances to both DM and CM noises. For DM noise, the inductance of two separate inductors is twice of that of a single inductor. For CM noise, the inductance of two separate inductors is half of that of a single inductor. The purpose of using separate inductors here is to suppress both DM and CM noises. L_{CM1} is 3.2 mH with 39.5-μH leakage, L_{DM1} is 40 μH, C_{CM1} is 100 nF, C_{CM2} is 47 nF, and C_1 and C_2 are 33 μF. The two separate inductors in the second stage have an inductance of 8 μH each. C_3 is 100 nF. The motor drive has a power of 3 kW with 300-V dc input and 12-kHz switching frequency. The measurement setup is the same as that shown in Fig. 2.

In the following experiments, before CM noise is measured, the mutual inductance between two CM noise loops will be first extracted using a similar method to that proposed in [19]. The extraction process is carried out when the motor drive is not running. Because only the mutual inductance between two CM noise loops is to be extracted, L_{CM1} and L_{DM1} are removed from the filter PCB. On the other hand, L_{CM2} and L_{DM2} are short-circuited using two short wires. The mutual inductance between the cable–motor and the output loop is ignored and not measured because the cable and motor are far from the output loop and are shielded. An Agilent balanced four-port network analyzer E5070B is used to measure the S-parameters of the CM noise network from IGBTs in the motor drive to the outputs of LISNs. The mutual inductance between two CM noise loops is extracted from the measured S-parameters.

After the mutual inductance between two CM noise loops is extracted, inductors are remounted to the filter PCB for CM noise measurement. A noise separator [2] is connected to the outputs of the LISNs. Two precision attenuators are used between the LISNs and the noise separator to guarantee that the noise separator is not saturated, and the output of the noise separator is connected to a spectrum analyzer to measure CM

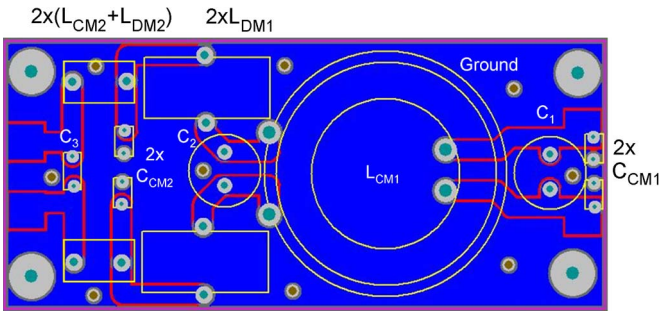

Fig. 16. EMI filter PCB layout with CM capacitors sharing the same grounding path.

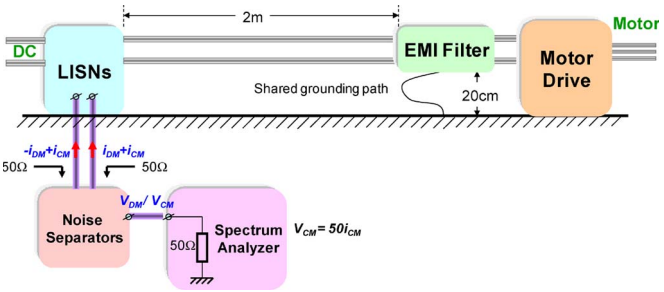

Fig. 17. EMI measurement setup: CM capacitors sharing the same grounding path.

noise. The experiments are carried out step by step, while CM noise is measured in each step.

In the first step, the CM noise of the motor drive is measured and recorded without any attenuation applied. The measured CM noise is shown in Fig. 19. In the second step, a two-stage EMI filter with CM capacitors sharing the same grounding path, as shown in Fig. 4, is connected between the motor drive and LISNs. The EMI filter's PCB layout is shown in Fig. 16. Both the top and bottom sides of the PCB have a copper plane, and the copper planes are grounded to the ground plane in the EMI measurement setup. All CM capacitors are soldered to these two grounded copper planes; hence, all CM capacitors share the same grounding path. The filter layout in Fig. 16 has considered the effects of possible couplings between CM filter components. Unlike a DM inductor, which is usually the leakage of a CM inductor so that its magnetic flux extends to air, a CM inductor's CM magnetic flux is confined in the core; thus, the coupling between a CM inductor and other CM components are not as significant as that in a DM inductor case. Furthermore, the CM capacitors used in this filter have a very small size and are far apart, and the couplings between the CM capacitors in two stages are also insignificant. Experiments will show that the parasitic parameters in grounding paths are the most important for the CM filter's performance. The magnetic material used for the CM inductor is J material (ferrite, $\mu_r = 5000$) from Magnetics Inc. Two windings are evenly distributed around the core; thus, their leakage inductance is small. The measurement setup is shown in Fig. 17. The mutual inductance between two CM noise loops, which is close to the self partial inductance of the grounding path as analyzed in previous section, is first extracted and shown in Fig. 18. Because the common grounding point of the system is far from the filter, the grounding wire is

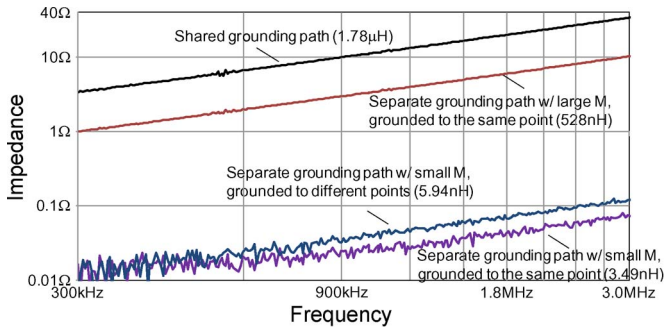

Fig. 18. Extracted impedance of mutual inductance between two CM noise loops.

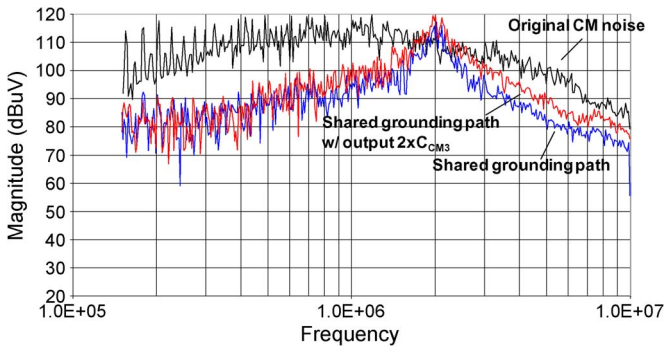

Fig. 19. Comparison of measured CM noise.

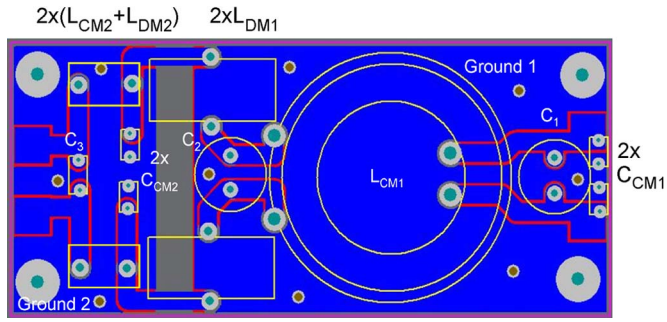

Fig. 20. EMI filter PCB layout with separate copper planes.

long. The extracted mutual inductance is around 1.8 μH. CM noise is then measured and shown in Fig. 19. Compared with the CM noise without EMI filters, it has up to 28-dB noise reduction at low frequencies. At high frequencies, the noise reduction is not as good as it is at low frequencies due to the effects of the mutual inductance (or the parasitic inductance of the grounding path) between two CM noise loops. In the third step, two 100-nF CM capacitors are added to the output of the filter such that the second-stage CM filter is a π-type filter like that shown in Fig. 5. The filter has an equivalent circuit that is the same as the circuit shown in Fig. 6. CM noise is measured and recorded in Fig. 19. Compared with the measurement in the last step, the CM noise is not reduced but increases from 450 kHz to 10 MHz, which verifies the analysis in Figs. 5 and 6.

In the fourth step, the two CM capacitors added in the third step are removed. The copper planes on both the top and bottom sides of the PCB are divided to two separate parts, and the CM capacitors on each stage are soldered to these two separate parts, respectively, as shown in Fig. 20. Two PCB copper plane

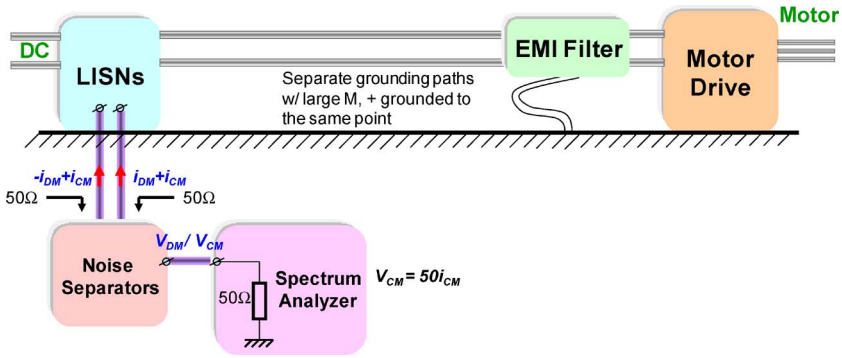

Fig. 21. EMI measurement setup: CM capacitors are grounded separately with large mutual inductance.

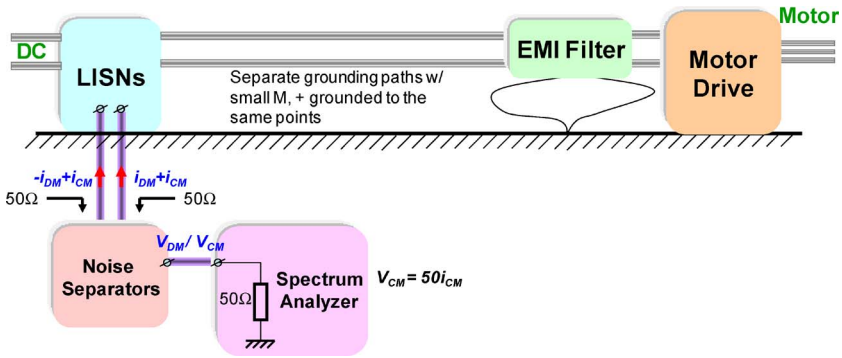

Fig. 22. EMI measurement setup: CM capacitors are grounded separately with small mutual inductance.

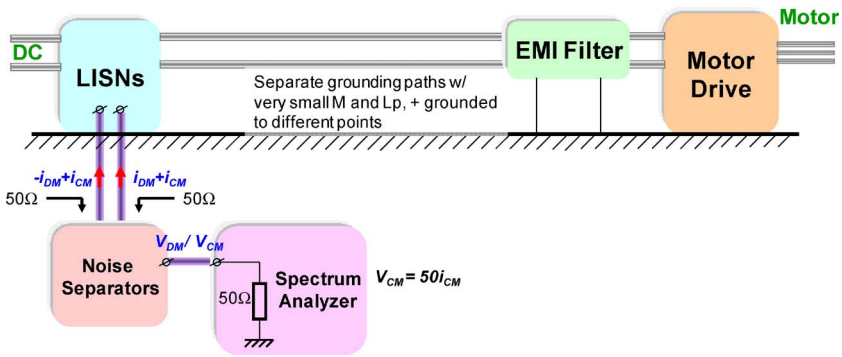

Fig. 23. EMI measurement setup: CM capacitors are grounded separately with very small inductance.

parts are grounded to the same point on the ground plane with two separate grounding paths, as shown in Fig. 7. The two grounding paths are close to each other, which results in a high mutual inductance between the two paths. This setup is shown in Fig. 21. The extracted mutual inductance between two CM noise loops is 528 nH, as shown in Fig. 18. CM noise is measured and shown in Fig. 24. There is only several decibels of improvement at low frequencies and even no improvement at high frequencies due to the effects of the mutual inductance between two grounding paths. This verifies the analysis in Figs. 7 and 8.

In the fifth step, the two grounding paths are kept far apart but they are still grounded to the same point, as shown in Fig. 22. The mutual inductance between the two grounding paths is therefore much smaller than the inductance that occurs in the fourth step. The extracted mutual inductance between two CM noise loops is only 3.49 nH, as shown in Fig. 18. The noise below 900 kHz is the background noise of the network analyzer. CM noise is also measured and shown in Fig. 24. There is a 20–30 dB improvement in the entire measured frequency range as compared with the results in Step 4 due to a smaller mutual inductance between two grounding paths than that in Step 4.

In the last step, the CM capacitors on each stage are grounded separately at different points on the ground plane, as shown in Fig. 9. The two grounding paths are kept short (the length is only 25% of that in previous steps) and are kept far away from each other. The extracted mutual inductance between two CM noise loops is 5.94 nH, as shown in Fig. 18. The noise below 900 kHz is the background noise of the network analyzer. The measurement setup is shown in Fig. 23. As analyzed in Section II, both the mutual inductance and the inductance of grounding paths are very small. Again, the CM noise is measured and shown in Fig. 24. It is here that the lowest noise is achieved. There is another improvement of up to 30 dB

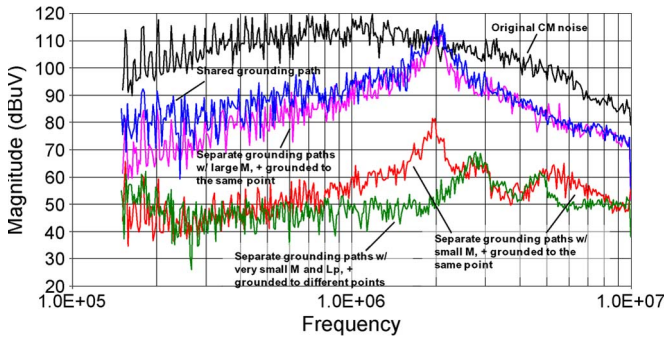

Fig. 24. Comparison of measured CM noise.

from the range of 300 kHz–2.4 MHz and up to a 15-dB improvement from 5 to 8 MHz as compared with the result in Step 5. Step 5 gives a smaller mutual inductance because the distance between two grounding paths is farther than that in the last step. Although the mutual inductance is a little bit larger than that in Step 5, the self partial inductance is much smaller (75% reduction is measured), and the CM noise can still be further reduced as described in (8). This verifies the analysis in Fig. 9.

In this section, simulations and experiments verified all the analyses in Section II. It has been verified that, for an EMI filter, different grounding patterns can result in a much different performance on CM noise reduction. The mutual inductance between two CM noise paths or loops is very critical to the CM noise suppression in power electronics systems. EMI filter structures in different power electronics systems could be different; however, the principles discussed in this paper still apply.

IV. Conclusion

This paper has theoretically analyzed the parasitic effects of grounding paths on the CM EMI filter's performance. It first proves that the CM capacitors should be grounded separately. If CM capacitors have to share the same grounding path, the output loop should not have CM capacitors. Because of the large difference in current between grounding paths, the mutual inductance between two grounding paths (CM noise loops) are detrimental to the CM filter's performance. Because of this, the mutual inductance should be as small as possible. The analysis is verified by both simulations and experiments.

Acknowledgment

This work made use of the Engineering Research Center Shared Facilities supported by the National Science Foundation (NSF) under NSF Award EEC-9731677 and the Industry Partnership Program.

References

[1] S. Wang, F. C. Lee, D. Y. Chen, and W. G. Odendaal, "Effects of parasitic parameters on EMI filter performance," *IEEE Trans. Power Electron.*, vol. 19, no. 3, pp. 869–877, May 2004.

[2] S. Wang, F. C. Lee, and W. G. Odendaal, "Characterization, evaluation and design of noise separator for conducted EMI noise diagnosis," *IEEE Trans. Power Electron.*, vol. 20, no. 4, pp. 974–982, Jul. 2005.

[3] R. Morrison, *Grounding and Shielding Techniques in Instrumentation*. New York: Wiley, 1977.

[4] R. Morrison, *Grounding and Shielding: Circuits and Interference*. Hoboken, NJ: Wiley-Interscience, 2007.

[5] E. Holzman, *Essentials of RF and Microwave Grounding*. Boston, MA: Artech House, 2006.

[6] K. Gulez, A. A. Adam, and H. Pastaci, "Torque ripple and EMI noise minimization in PMSM using active filter topology and field-oriented control," *IEEE Trans. Ind. Electron.*, vol. 55, no. 1, pp. 251–257, Jan. 2008.

[7] R. L. Ozenbaugh, *EMI Filter Design*, 2nd ed. New York: Marcel Dekker, 2001.

[8] M. J. Nave, *Power Line Filter Design for Switched-Mode Power Supply*. New York: Van Nostrand, 1991.

[9] H. W. Ott, *Noise Reduction Techniques in Electronic Systems*, 2nd ed. New York: Wiley, 1988.

[10] R. O'Riley, *Electrical Grounding*, 6th ed. Clifton Park, NY: Delmar Cengage Learning, 2001.

[11] S. Wang, F. C. Lee, and J. D. van Wyk, "Effects of interactions between filter parasitics and power interconnects on EMI filter performance," *IEEE Trans. Ind. Electron.*, vol. 54, no. 6, pp. 3344–3352, Dec. 2007.

[12] H.-I. Hsieh, J.-S. Li, and D. Chen, "Effects of X capacitors on EMI filter effectiveness," *IEEE Trans. Ind. Electron.*, vol. 55, no. 2, pp. 945–955, Feb. 2008.

[13] M. M. Hernando, A. Fernandez, M. Arias, M. Rodriguez, Y. Alvarez, and F. Las-Heras, "EMI radiated noise measurement system using the source reconstruction technique," *IEEE Trans. Ind. Electron.*, vol. 55, no. 9, pp. 3258–3265, Sep. 2008.

[14] L. A. Barragan, D. Navarro, J. Acero, I. Urriza, and J. M. Burdio, "FPGA implementation of a switching frequency modulation circuit for EMI reduction in resonant inverters for induction heating appliances," *IEEE Trans. Ind. Electron.*, vol. 55, no. 1, pp. 11–20, Jan. 2008.

[15] E. Clavel, J. Roudet, T. Chevalier, and D. M. Postariu, "Modeling of connections taking into account return plane: Application to EMI modeling for railway," *IEEE Trans. Ind. Electron.*, vol. 56, no. 3, pp. 678–684, Mar. 2009.

[16] K. Jalili and S. Bernet, "Design of LCL filters of active-front-end two-level voltage-source converters," *IEEE Trans. Ind. Electron.*, vol. 56, no. 5, pp. 1674–1689, May 2009.

[17] M. L. Heldwein and J. W. Kolar, "Design of minimum volume EMC input filters for an ultra compact three-phase PWM rectifier," in *Proc. 9th COBEP*, Sep. 30–Oct. 4, 2007, pp. 454–461.

[18] C. R. Paul, *Introduction to Electromagnetic Compatibility*, 2nd ed. Hoboken, NJ: Wiley, 2006.

[19] S. Wang, F. C. Lee, and W. G. Odendaal, "Characterization and parasitic extraction of EMI filters using scattering parameters," *IEEE Trans. Power Electron.*, vol. 20, no. 2, pp. 502–510, Mar. 2005.

Shuo Wang (S'03–M'06–SM'07) received the B.S.E.E. degree from Southwest Jiaotong University, Chengdu, China, in 1994, the M.S.E.E. degree from Zhejiang University, Hangzhou, China, in 1997, and the Ph.D. degree from the Center for Power Electronics Systems (CPES), Virginia Polytechnic Institute and State University, Blacksburg, in 2005.

He has been with the Department of Electrical and Computer Engineering, The University of Texas at San Antonio since 2010. He was with the Electrical Power Systems Group, GE Aviation Systems, Vandalia, OH, from 2009 to 2010. He was a Research Assistant Professor at CPES from 2005 to 2009. From 1997 to 1999, he was with ZTE Telecommunication Corporation, Shenzhen, China. In 2000, he was with UTStarcom Telecommunication Corporation, Hangzhou. He is the holder of four U.S. patents and has two others pending. He has published more than 70 academic papers in IEEE Transactions and conference proceedings. His research interests include electromagnetic interference/electromagnetic compatibility in power electronics systems, high-density power conversion, three-phase power conversion and inversion, motor drives, generator control, and power systems.

Dr. Wang is an Associate Editor for the IEEE Transactions on Industry Applications. He was the recipient of the 2005 Best Transactions Paper Award from the IEEE Transactions on Power Electronics and the William M. Portnoy Award for the best paper presented at the IEEE Industry Applications Society Annual Conference in 2004.

Yoann Yorrick Maillet received the B.S. degree in electrical engineering and the M.S. degree from Virginia Polytechnic Institute and State University (Virginia Tech), Blacksburg, in 2006 and 2008, respectively.

He joined the Center for Power Electronics Systems, Virginia Tech. His research interests include passive electromagnetic-interference (EMI) filter design and integrated EMI choke for common-mode and differential-mode supressions. Since 2008, he has been an Electrical Engineer with Converteam, Inc., Pittsburgh, PA, a power-conversion company specializing in drives, controls, motors, and generators.

Fei (Fred) Wang (S'85–M'91–SM'99–F'10) received the B.S. degree in electrical engineering from Xi'an Jiaotong University, Xi'an, China, in 1982, and the M.S. and Ph.D. degrees in electrical engineering from the University of Southern California, Los Angeles, in 1985 and 1990, respectively.

He was a Research Scientist in the Electric Power Laboratory, University of Southern California, from 1990 to 1992. He joined the GE Power Systems Engineering Department, Schenectady, NY, as an Application Engineer in 1992. From 1994 to 2000, he was a Senior Product Development Engineer with GE Industrial Systems, Salem, VA. During 2000 to 2001, he was the Manager of the Electronic and Photonic Systems Technology Laboratory, GE Global Research Center, Schenectady, and Shanghai, China. In 2001, he joined the Center for Power Electronics Systems (CPES), Virginia Polytechnic Institute and State University, Blacksburg, VA, as a Research Associate Professor and became an Associate Professor in 2004. Since 2003, he has also served as the CPES Technical Director. In 2009, he joined The University of Tennessee, Knoxville, TN, and Oak Ridge National Laboratory, Oak Ridge, TN, as Condra Chair Professor in Power Electronics. His interests include power electronics, power systems, controls, electric machines, and motor drives.

Rixin Lai (S'07–M'10) received the B.S. and M.S. degrees in electrical engineering from Tsinghua University, Beijing, China, and the Ph.D. degree from the Center for Power Electronics Systems, Virginia Polytechnic Institute and State University, Blacksburg, in 2002, 2005, and 2008, respectively.

In 2009, he joined the Electronic Power Conversion Laboratory, GE Global Research Center, General Electric Company, Niskayuna, NY. His research interests include passive filter design, electromagnetic interference technology, modeling and control of three-phase converters, and high power density converter development.

Fang Luo (S'06) was born in Wuhan, China. He received the B.S. degree from Huazhong University of Science and Technology, Wuhan, China, in 2003.

He has been in the direct Ph.D. program since 2005. Since 2007, he has been with the Center for Power Electronics Systems (CPES), Virginia Polytechnic Institute and State University (Virginia Tech), Blacksburg, as a Visiting Student, supported by the Chinese Scholarship Council and CPES. His experience in power electronics includes research and development on uninterrupted-power-supply systems, battery monitoring and management systems, and dc power distribution network protection. His current topic is high-density electromagnetic-interference (EMI) filtering solutions and passive EMI filter integration in motor-drive systems.

Dushan Boroyevich (S'81–M'86–SM'03–F'06) received the Dipl.Ing. degree from the University of Belgrade, Belgrade, Serbia, in 1976, the M.S. degree from the University of Novi Sad, Novi Sad, Serbia, in 1982, and the Ph.D. degree from Virginia Polytechnic Institute and State University (Virginia Tech), Blacksburg, in 1986.

From 1986 to 1990, he was an Assistant Professor and the Director of the Power and Industrial Electronics Research Program, Institute for Power and Electronic Engineering, University of Novi Sad, and, later, as an acting Head of the institute. He then joined The Bradley Department of Electrical and Computer Engineering, Virginia Tech, as an Associate Professor, where he is currently the American Electric Power Professor of the department and a Codirector of the Center for Power Electronics Systems. His research interests include multiphase power conversion, electronic power distribution systems, power electronics systems modeling and control, and multidisciplinary design optimization.

Dr. Boroyevich was a recipient of the IEEE William E. Newell Power Electronics Technical Field Award.